

# Peripheral interactions of relativistic $^{14}\text{N}$ nuclei with emulsion nuclei

T. V. Shchedrina,<sup>\*</sup> V. Bradnova, A. D. Kovalenko, A. I. Malakhov,  
P. A. Rukoyatkin, V. V. Rusakova, P. I. Zarubin,<sup>†</sup> and I. G. Zarubina  
*Joint Institute for Nuclear Research, Dubna, Russia*

M. M. Chernyavsky, S. P. Kharlamov, and G. I. Orlova  
*Lebedev Institute of Physics, Russian Academy of Sciences, Moscow, Russia*

M. Haiduc  
*Institute of Space Sciences, Magurele, Romania*

S. Vokál and A. Vokálová  
*P. J. Šafárik University, Košice, Slovak Republic*

(Dated: October 30, 2018)

## Abstract

The results of investigations of the dissociation of a  $^{14}\text{N}$  nucleus of momentum 2.86 A GeV/c in photo-emulsion are presented. The main characteristics of these reactions, that is the cross sections for various fragmentation channels, are given. The fragmentation was analyzed by means of an invariant approach. The momentum and correlation characteristics of  $\alpha$  particles for the  $^{14}\text{N} \rightarrow 3\alpha + \text{X}$  channel in the laboratory system and the rest systems of  $3\alpha$  particles were considered. The results obtained for the  $^{14}\text{N}$  nucleus are compared with similar data for the  $^{12}\text{C}$  and  $^{16}\text{O}$  nuclei.

PACS numbers: 21.45.+v, 23.60.+e, 25.10.+s

---

<sup>\*</sup>Electronic address: shchedrina@lhe.jinr.ru

<sup>†</sup>Electronic address: zarubin@lhe.jinr.ru; URL: <http://becquerel.lhe.jinr.ru>

## I. INTRODUCTION

The fragmentation of relativistic nuclei is a source of information about their structure. The nuclear photo-emulsion method makes it possible to study in detail the fragmentation of a projectile thanks to a high resolution capability of emulsion and the detection of secondaries in a  $4\pi$  geometry. The registration of all charged particles and their identification enable one to explore the isotopic composition of fragments and the projectile fragmentation channels. In the present paper, we give a detailed examination both of the decays conventionally called “white” starts because they have no target-nucleus fragments and of the decays involving the production of several target-nucleus fragments. The main criterion for selecting the appropriate events used for the study of the projectile fragmentation is the requirement of conservation of the primary charge in a narrow fragmentation cone and the absence of produced charged particles.

## II. EXPERIMENT

A stack of layers of BR emulsion of a relativistic sensitivity was exposed to a beam of  $^{14}\text{N}$  nuclei accelerated to a momentum of 2.86 A GeV/c at the Nuclotron of the Laboratory of High Energy Physics (JINR). The layer thickness and dimensions were  $600\mu\text{m}$  and  $10\times 20\text{ cm}^2$ , respectively. The exposed beam was pointed parallel to the emulsion plane along its long side. Events were sought by viewing over the track length which provided the accumulation of statistics without selection. This made it possible to determine the mean free path of  $^{14}\text{N}$  interactions in emulsion. The fragment emission angles were measured by the microscope MPE-11 (Moscow, FIAN). Coordinate sensors were set on the X, Y, and Z axes to transmit information to a personal computer which provided its processing. The  $Z=1$  projectile fragments were separated from the  $Z=2$  fragments by sight because a single ionization of relativistic single-charged particles is reliably discriminated from a four-fold ionization of particles with charge 2. Fragments with  $Z=3,\dots,7$  were separated by counting  $\delta$  electrons. The momenta of single- and two-charged fragments with emission angles up to  $4\times$  were determined from multiple coulomb scattering measurements. The results of these measurements were utilized to identify the hydrogen and helium isotopes involved in the  $^{14}\text{N}$  fragment composition.

TABLE I: The mean free path of  $\lambda$  in nuclear emulsion

<i>Nuclei</i>	$p_0$ , A GeV/c	$\lambda_{theor}$ , cm.	$\lambda_{exp}$ , cm.	Ref.
$^4\text{He}$	4.5	19.6	$19.5 \pm 0.3$	[1]
$^6\text{Li}$	4.5	16.5	$14.1 \pm 0.4$	[1]
$^7\text{Li}$	3.0	15.9	$14.3 \pm 0.4$	[2]
$^{12}\text{C}$	4.5	13.5	$13.7 \pm 0.5$	[1]
$^{14}\text{N}$	2.9	13.0	$13.0 \pm 0.4$	present paper
$^{16}\text{O}$	4.5	12.1	$13.0 \pm 0.5$	[1]
$^{22}\text{Ne}$	4.1	10.6	$10.2 \pm 0.1$	[1]
$^{24}\text{Mg}$	4.5	10.0	$9.6 \pm 0.4$	[1]

### III. THE MEAN FREE PATH OF INTERACTIONS

On the viewed track length of 123.21 m we found 960 events of interactions of the  $^{14}\text{N}$  nucleus with the emulsion nuclei. Thus the mean free path of a  $^{14}\text{N}$  in emulsion is  $\lambda_N = (13 \pm 0.4)\text{cm}$ . This value and the  $\lambda_A$  values for a number of other projectiles in emulsion obtained earlier in [1],[2] are displayed in Table I in which there are also the  $\lambda_A$  values calculated by the Bradt-Peters equation [3].

### IV. TOPOLOGY IN THE RELATIVISTIC $^{14}\text{N}$ FRAGMENTATION

Of 950 interactions found, we selected events in which the total fragment charge was equal to the  $Z_0=7$  fragment charge and there were no produced particles. The selected events are divided in two classes. The events of the type of “white” star (44 events) and the interactions involving the production of one or a few target-nucleus fragments (61 events) belong to the first class. The name “white” is a conventional one that refers to the interactions in which there are neither target fragments nor produced particles. They are produced in case when the energy transferred to a fragmenting nucleus is minimal which leads to a distraction of inter-cluster bounds but, as a rule, the bounds inside the clusters remain unaffected. This is the reason for which they are of special interest for the study of the cluster structure of nuclei. The other class of events, we are interested in, reveals a simultaneous breakup of

TABLE II: The charge topology distribution of the “white”stars and the interactions involving the target-nucleus fragment production in the  $^{14}\text{N}$  dissociation at 2.86 A GeV/c momentum.

$Z_{fr}$	6	5	5	4	3	3	–	–
$N_{Z=1}$	1	–	2	1	4	2	3	1
$N_{Z=2}$	–	1	–	1	–	1	2	3
$N_{W.S.}$	13	4	3	1	1	1	6	15
$N_{t.f.}$	15	1	3	3	–	2	5	32
$N_{\Sigma}$	28	5	6	4	1	3	11	49
$N_{\Sigma,\%}$	26	5	5	4	1	3	10	46

both interacting nuclei which results in the production of target-nucleus fragments. The projectile fragments are emitted mainly within a narrow forward cone the opening angle of which is described by the relation (1)

$$\sin\Theta_f = \frac{0.2 \text{ GeV}/c}{p_0} \quad (1)$$

where 0.2 GeV/c is the value of the Fermi momentum and  $p_0$  the momentum per nucleon of the projectile. In our case, at  $p_0=2.86$  A GeV/c the fragmentation angle is  $4^\circ$ .

Table II shows the charge multi-fragmentation topology which was studied for the events satisfying the above-mentioned conditions. The upper line is the  $Z>2$  fragment charge, the second line is the number of single-charged fragments, the third one the number of two-charged fragments, and the fourth and fifth lines are the number of the detected events with a given topology for “white”stars and events with target-nucleus excitation for each channel, respectively. The two last lines present the total number of interactions calculated in absolute values and in percent.

The analysis of the data of Table II shows that the number of channels involving  $Z>3$  fragments for the “white”stars is larger by about a factor of 1.5 than that for the events accompanied by a target breakup. On the contrary, for the 2+2+2+1 charge configuration channel this number is smaller by about a factor of 1.5. Thus, in the events with target breakup, the projectile fragments more strongly than in the “white”stars. The data of Table II points to the predominance of the channel with the 2+2+2+1 charge configuration (49 events) which has been studied in more detail. The mean free path for this channel

$\lambda_{3He+H}(^{14}N)=2.5\pm0.36$  m. An analogous value for the carbon nucleus is larger by a factor of 4,  $\lambda_{3He}=10.3\pm1.9$  m. The obtained results show that the  $^{14}N$  nucleus constitutes a very effective source for the production of  $3\alpha$  system.

The hydrogen and helium isotopes were separated basing on the results of measurements of their momenta ( $p\beta c$ ) under the assumption that the spectator target-nucleus fragments conserve their momentum per nucleon which is equal to the primary one, that is,  $A_{fr}=p\beta c_{exp}/p_0\beta c$ . The multiple coulomb scattering method used for the determination of the momenta is based on the suggestion that the rms of a  $<|D|>$  over a cell length of  $t$  is associated with the  $p\beta c$  value by the equation (2)

$$<|D|>= \frac{Z_f \cdot K \cdot t^{\frac{3}{2}}}{573 \cdot p\beta c} \quad (2)$$

where  $Z$  is the charge,  $p$  the momentum,  $\beta c$  the particle velocity, and the scattering constant the value of which is known. Distortions and a false scattering were taken into account by a so-called  $\rho$  method [6]. In multiple coulomb scattering the  $p\beta c$  distribution for individual particles with the same charge and momentum must be close to the normal one. Therefore the  $p\beta c$  distribution for a group of fragments with identical velocity and charge, but with different masses, must be a superposition of several normal distributions. Fig. 1(a,b) presents the results of measurements of a multiple-particle scattering for single- and doubly-charged fragments, respectively. The measured momenta for single-charged fragments are well approximated by the sum of two Gaussians the peaks of which are located at 2.6 GeV/c and 5.6 GeV/c and correspond to  $^1H$  and  $^2H$  isotopes Fig. 1(a). The ratio of the  $^1H$  and  $^2H$  isotope yields thus obtained is nearly 2:1. This points out that, in our case, the deuteron fraction is seen to be noticeably smaller as compared to the cases of the relativistic  $^6Li$  (2+1 channel) and  $^{10}B$  (2+2+1 channel) fragmentation where the proton and deuteron yields are about the same.

Fig. 1(b) gives the measured  $p\beta c$  distribution for 37 double-charged fragments. This distribution is satisfactorily approximated by the sum of two normal distributions which is shown by the continuous line. The approximating distribution peaks correspond to the values 7.8 and 11.3 which are rather close to the  $p\beta c$  values which relate to the  $^3He$  and  $^4He$  isotopes. The fragment yield for  $^3He$  is about 40% and for  $^4He$  - 60%. There are also a few He isotopes (5% of the total number of interactions) in the  $p\beta c$  range from 14 to 16 MeV that were identified as  $^6He$ . The events involving the  $^6He$  production are planned to

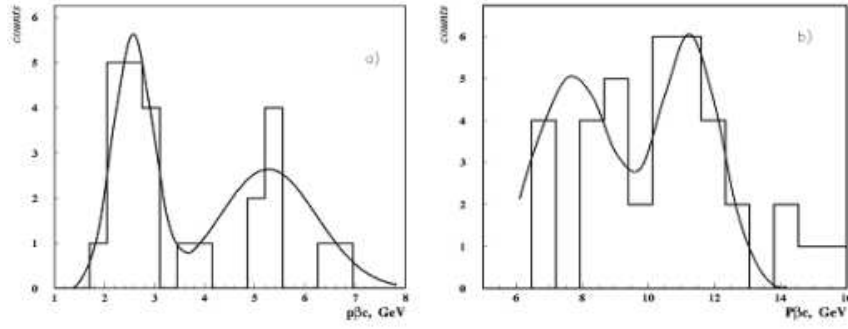


FIG. 1: Momentum separation of single- a) and double- b) charged fragments according to  $p\beta c$  measurements for the  $^{14}\text{N}$  nucleus of a momentum of 2.86 A GeV/c. The continuous line is a Gaussian description by the least square method.

be analyzed in more detail.

## V. MOMENTUM AND CORRELATION CHARACTERISTICS OF $\text{N}\alpha$ PARTICLE SYSTEMS

We go over to the consideration of the main kinematic characteristics of relativistic  $\alpha$  particles, the projectile fragments, from the  $^{14}\text{N} \rightarrow 3\alpha + \text{X}$  reaction and we compare these characteristics with those from the  $^{12}\text{C} \rightarrow 3\alpha$  and  $^{16}\text{O} \rightarrow 4\alpha$  reactions. Fig. 2(a) displays the squared transverse momentum distribution of  $\alpha$  particles in the laboratory system for the channel  $^{14}\text{N} \rightarrow 3\alpha + \text{X}$ . The transverse momenta  $P_T$  are calculated by the equation (3)

$$P_T = p_0 \cdot A \cdot \sin\theta \quad (3)$$

that is, the analysis of  $P_T$  distributions implies virtually an analysis of  $\alpha$  particle angular distributions. This distribution has a break at  $P_T^2 = 0.05 \text{ (GeV/c)}^2$ . The continuous line is the sum of two Rayleigh distributions.

The values of the momenta in a 3  $\alpha$  particle system can be obtained by (subtraction) taking into account the momentum which is acquired by the interacting system:

$$\mathbf{P}_{\text{Ti}}^* \cong \mathbf{P}_{\text{Ti}} - \frac{\sum \mathbf{P}_{\text{Ti}}}{3} \quad (4)$$

The  $P_T$  distribution for  $\alpha$  particles in  $^{14}\text{N} \rightarrow 3\alpha + \text{X}$  reactions is given in Fig. 2(b). The average  $P_T^*$  values were expected to be much smaller than the  $P_T$  values in the laboratory system and identical for  $^{14}\text{N}$ ,  $^{12}\text{C}$  [4],  $^{16}\text{O}$  [5] within errors.

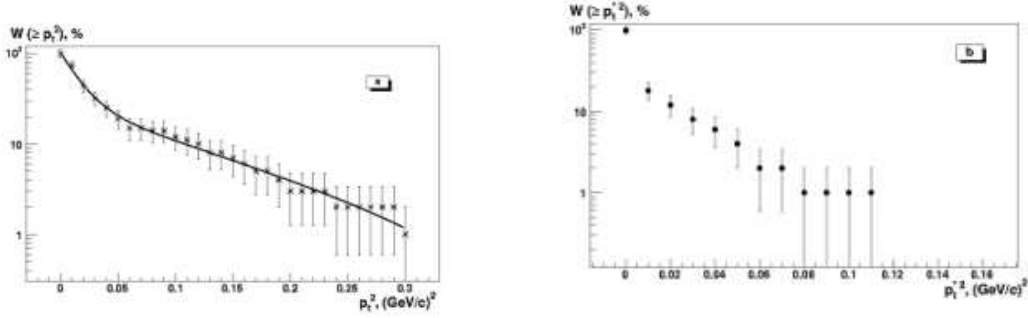


FIG. 2: The  $P_T^2$  lab.system (a) and  $P_T^{*2}$   $3\alpha$  particle rest system(b) distributions (channel  $^{14}\text{N} \rightarrow 3\alpha + X$ ). The continuous line of Fig. 2a is the sum of two Relay distributions.

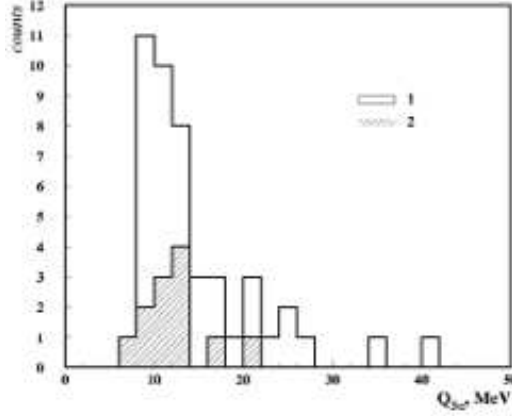


FIG. 3: The invariant excitation energy  $Q_{3\alpha}$  distribution of three  $\alpha$  particles with respect to the  $^{12}\text{C}$  ground state for the process  $^{14}\text{N} \rightarrow 3\alpha + X$ . The following notation is used: 1) all the events of the given dissociation, 2) “white” stars.

In order to estimate the energy scale of production of  $3\alpha$  particle systems in the  $^{14}\text{N} \rightarrow 3\alpha + X$  channel, we present the invariant excitation energy  $Q$  distribution with respect to the  $^{12}\text{C}$  ground state:

$$Q = M^* - M \quad (5)$$

where  $M$  is the mass of the ground state corresponding to the charge and the weight of the system being analyzed,  $M^*$  the invariant mass of the system of fragments.

$$M^{*2} = -(\sum P_j)^2$$

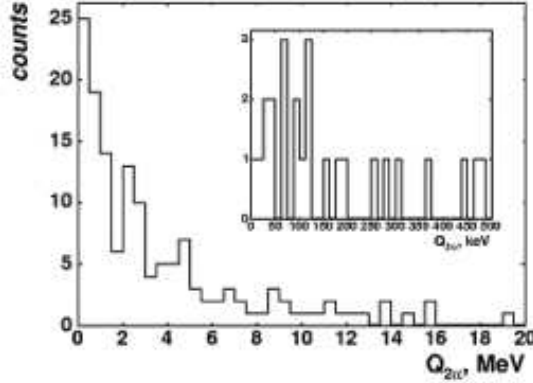


FIG. 4: The invariant excitation energy  $Q_{2\alpha}$  distribution of  $\alpha$  particle pairs for the process  $^{14}\text{N} \rightarrow 3\alpha + \text{X}$ . In the inset: a fraction of the distribution at 0-500 keV.

,  $P_j$  the 4-momenta of the  $j$  fragments.

The main part of the events is concentrated in the  $Q$  area from 10 to 14 MeV, covering the known  $^{12}\text{C}$  levels (Fig. 3). Softening of the conditions of the  $3\text{He} + \text{H}$  selection, for which the target fragment production is allowed, does not result in a shift of the  $3\alpha$  excitation peak. This fact suggests the universality of the  $3\alpha$  state population mechanism.

To estimate the fraction of the events involving the production of an intermediate  $^8\text{Be}$  nucleus in the reactions  $^{14}\text{N} \rightarrow ^8\text{Be} + \text{X} \rightarrow 3\alpha + \text{X}$  we present the invariant excitation energy distribution for an  $\alpha$  particle pair with respect to the  $^8\text{Be}$  ground state (Fig. 4). The first distribution peak relates to the value to be expected for the decay products of an unstable  $^8\text{Be}$  nucleus in the ground state  $0^+$ . This part of the spectrum increased by a factor of 20 is presented in the inset of Fig. 4. The distribution centre is seen to coincide well with the decay energy of the  $^8\text{Be}$  ground state. The fraction of the  $\alpha$  particles originating from the  $^8\text{Be}$  decay is 25-30%.

The role of  $^8\text{Be}$  is clearly pronounced in a strongly asymmetric  $\varepsilon_{ij}^*$  distribution of  $\alpha$  particle pairs in the rest system of the  $3\alpha$  particles of the nucleus  $^{14}\text{N} \rightarrow 3\alpha + \text{X}$  (Fig. 5). The asymmetry of the asymuthal angle  $\varepsilon_{ij}^*$  is also revealed for alpha fragments in the c.m.s. due to  $^{12}\text{C}$  [4] and  $^{16}\text{O}$  [5] decays. The values of the coefficients of asymuthal asymmetry and collinearity coincide within errors for  $^{14}\text{N}$  and  $^{12}\text{C}$  and they considerably differ the  $^{16}\text{O} \rightarrow 4\alpha$  decay. This may be explained by a more complicated combinatority of  $\alpha$  particles for the

latter nucleus, as well as by the fact that  $\alpha$  fragments can also be decay products of other intermediate unstable objects.

## VI. CONCLUSION

In conclusion we summarize the main results of the present paper. We give the results of the study of the dissociation of  $^{14}\text{N}$  nuclei of a primary momentum of 2.86 GeV/c per nucleon in their interactions with the emulsion nuclei. The charge topology distribution indicates the leading role of the 2+2+2+1 charge configuration channel.

Preliminary data show that for the  $^{14}\text{N} \rightarrow 3\alpha + \text{H}$  channel the relation of the protons and neutrons  $N_p:N_d \approx 2$ , and the relation of the helium isotopes  $^4\text{He}:^3\text{He} \approx 1.5$ . There are also a few helium isotopes (5% of the total number of interactions) identified as  $^6\text{He}$ . A more detailed analysis is needed here.

The  $\varepsilon_{ij}^*$  distribution in the c.m.s. of  $\alpha$  fragments for  $^{14}\text{N}$ ,  $^{12}\text{C}$ , and  $^{16}\text{O}$  are asymmetric with an abundance at  $140^\circ - 180^\circ$ .

The energy scale of the  $3\alpha$  system production has been estimated. According to the available statistics 80% of interactions are concentrated at 10-14 MeV. The fraction of the  $^{14}\text{N} \rightarrow ^8\text{Be} + \text{X} \rightarrow 3\alpha + \text{X}$  channel involving the production of an intermediate  $^8\text{Be}$  nucleus is about 25%.

## Acknowledgments

The work was supported by the Russian Foundation for Basic Research ( Grants 96-159623, 02-02-164-12a, 03-02-16134, 03-02-17079 and 04-02-16593 ), VEGA 1/9036/02. Grant from the Agency for Science of the Ministry for Education of the Slovak Republic and the Slovak Academy of Sciences, and Grants from the JINR Plenipotentiaries of the Republic of Bulgaria, the Slovak Republic, the Czech Republic and Romania in the years 2002-2005.

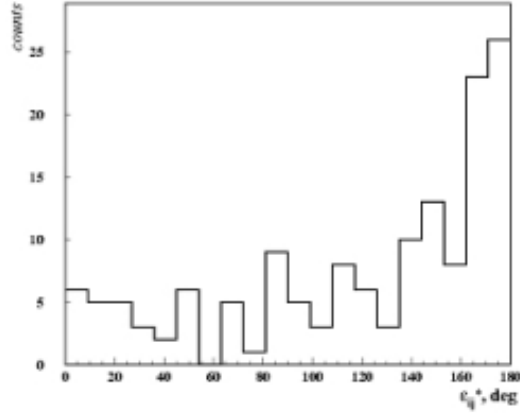


FIG. 5: The asymuthal angle  $\varepsilon_{ij}^*$  distribution in the rest system of  $3\alpha$  particles for the process  $^{14}\text{N} \rightarrow 3\alpha + \text{X}$ .

- 
- [1] M. I. Adamovich et al., Phys. At. Nucl., **62**, 1378-1387 (1999).
  - [2] M. I. Adamovich et al., J. Phys. G, **30**, 1479-1485 (2004).
  - [3] H. Bradt, B. Peters, Phys.Rev., **77**, 54 (1950).
  - [4] V. V. Belaga et al., Phys. At. Nucl., **58**, 1905-1910 (1995).
  - [5] F. A. Avetyan et al., Phys. At. Nucl., **59**, 110-116 (1996).
  - [6] Web site of the BECQUEREL Project, <http://becquerel.jinr.ru/>, or <http://pavel.lhe.jinr.ru/>